Langmuir

Article

pubs.acs.org/Langmuir

A Mass-Tagging Approach for Enhanced Sensitivity of Dynamic Cytokine Detection Using a Label-Free Biosensor

Sunmin Ahn,[†] David S. Freedman,[‡] Paola Massari,[§] Mario Cabodi,[†,∥] and M. Selim Ünlü*[,†,‡]

[†]Department of Biomedical Engineering, Boston University, Boston, Massachusetts 02215, United States

[‡]Department of Electrical and Computer Engineering, Boston University, Boston, Massachusetts 02215, United States

[§]Department of Medicine, Section of Infectious Diseases, Boston University School of Medicine, Boston, Massachusetts 02118, United States

[∥]Center for Nanoscience and Nanobiotechnology, Boston University, Boston, Massachusetts 02215, United States

Supporting Information

ABSTRACT: Monitoring cytokine release by cells allows the investigation of cellular response to specific external stimuli, such as pathogens or candidate drugs. Unlike conventional colorimetric techniques, label-free detection of cytokines enables studying cellular secretions in real time by eliminating additional wash and labeling steps after the binding step. However, label-free techniques that are based on measuring mass accumulation on a sensor surface are challenging for measuring small cytokines binding to much larger capture agents (usually antibodies) because the relative signal change is small. This problem is exacerbated when the capturing antibodies desorb from the surface, a phenomenon that almost inevitably occurs in immunoassays but is rarely accounted for. Here, we demonstrate a quantitative dynamic detection of interleukine-6 (IL-6), a pro-inflammatory cytokine, using an interferometric reflectance imaging sensor (IRIS). We improved the accuracy of the quantitative analysis of this relatively small protein (21 kDa) by characterizing the antibody desorption rate and compensating for the antibody loss during the binding experiment. By correcting for protein desorption, we achieved an analytical limit of detection at 19 ng/mL IL-6 concentration. We enhanced the sensitivity by 7-fold by using detection antibodies that recognize a different epitope of the cytokine. We demonstrate that these detection antibodies, which we call "mass tags", can be used concurrently with the target analyte to eliminate an additional wash and binding step. Finally, we report successful label-free detection of IL-6 in cell culture medium (with 10% serum) with comparable signal to that obtained in PBS. This work is the first to report quantitative dynamic label-free detection of small protein in a complex biological fluid using IRIS.

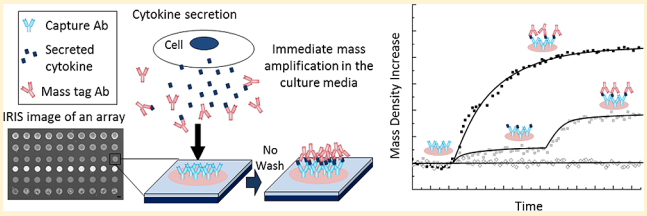

1. INTRODUCTION

Cytokines are a group of small proteins that participate in intercellular communications. They are secreted by a number of different cells and have a wide range of physiological functions.[1−4] Cytokines play particularly critical roles in inflammatory responses; thus, there is a great deal of interest in investigating cytokine production for pathology or monitoring disease progression and responses to drugs.[5] Cytokine expression levels are studied in numerous inflammatory conditions, such as rheumatoid arthritis and inflammatory bowel disease.[6,7] In addition, cytokines produced in the tumor microenvironment have been found to influence carcinogenesis.[8,9] Traditionally, cytokine detection is performed using enzyme-linked immunosorbent assay (ELISA) or enzyme-linked immunospot (ELISPOT). Both methods utilize sandwich immunoassays followed by detection of chemiluminescent or fluorescent molecules. Although these techniques are sensitive and robust, they are labor-intensive and time-consuming. More importantly, the labeling approaches do not allow a real-time detection of cytokines and presents limitations in kinetic analysis because their measurements are necessarily end-point.

Several label-free approaches for real-time cytokine detection have been reported using microring resonators, electrochemical sensors, and surface plasmon resonance (SPR) sensors.[10−14] In order to screen a large number of analytes in parallel, large arrays of sensors have been developed to be used in conjunction with an imaging modality to acquire data from the entire array.[15−17] For many label-free sensors, quantification of biomolecular interactions assumes that any change in mass accumulating on the sensor surface is a direct result of the binding events on the said surface. Thus, it is imperative that the sensor surface be stable during the biomolecular interactions to ensure an accurate quantitative analysis. Recently, we have investigated the effect of substrate erosion on microarrays during biochemical reactions and quantified the glass dissolution to improve the accuracy of label-free analysis.[18] In addition to the substrate stability, another factor that can

Received: August 20, 2012
Published: April 2, 2013

   dx.doi.org/10.1021/la400982h | *Langmuir* 2013, 29, 5369−5376

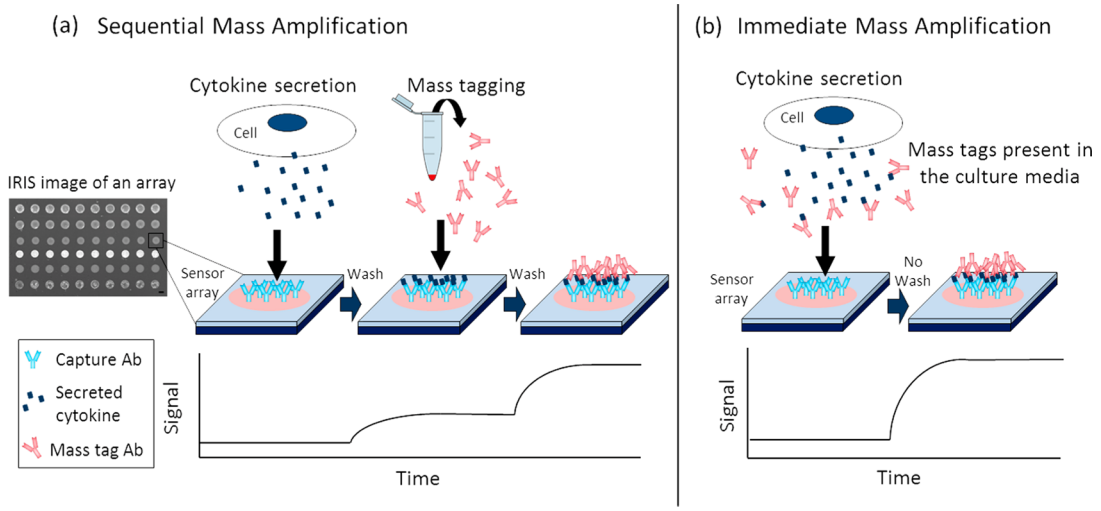

Figure 1. Schematic representations of utilizing mass tags to amplify binding signal of label-free biosensor. (a) Cell secreted cytokines are captured by the sensor array. After the initial binding of cytokine and washing of the array, the signal can be amplified by adding antibodies (mass tags) specific for the bound target. (b) With mass tagging antibodies present in the culture medium where cytokine is secreted, the cytokine mass is immediately amplified as the molecules are secreted, prior to binding. No wash is needed. Elimination of the wash step enables real-time detection with amplified signal.

significantly affect sensor performance is the stability of the capturing antibody density. Any desorption of the antibodies, resulting in a reduced surface density of capturing molecules, or probes, can easily lead to false negatives.[18] The error caused by probe desorption during binding events can be more pronounced in the case of cytokine detection. Because cytokines are much smaller than the capturing antibodies, any change in surface density of the antibodies can be detrimental in detecting signal changes. Additionally, each type of antibody is likely to have a specific desorption behavior, as evidenced by different immobilization behaviors,[19] making this challenge particularly significant for high-throughput applications, where multiple types of antibodies are used as capture probes.

In this work, we report on a real-time label-free detection of interleukin-6 (IL-6), an inflammatory mediator of 21 kDa mass, using an interferometric reflectance imaging sensor (IRIS).[17,20] We investigate the stability of the sensor surface by characterizing the desorption rate of the immobilized antibodies. These measured desorption rates are then used to correct the signal during IL-6 detection, resulting in a limit of detection (LOD) at 19 ng/mL of IL-6 concentration. The sensitivity is further improved by introducing a "mass tag", an antibody that recognizes a different epitope of the cytokine, achieving an LOD at 2.7 ng/mL of IL-6 concentration. This is a similar approach to traditional sandwich immunoassays, except that the final luminescence labeling step is eliminated as shown in Figure 1a. Furthermore, we demonstrate the detection of IL-6/anti-IL-6 antibody complex, where the mass tag is presented in the analyte solution prior to the binding on the surface as shown in Figure 1b. The complex detection presents a 7-fold improvement in signal, and this approach eliminates the stepwise addition of the mass tag. Finally, we present IL-6 detection in cell culture medium that contained recombinant human IL-6 standards.

2. EXPERIMENTAL SECTION

Dynamic Detection with Interferometric Reflectance Imaging Sensor (IRIS). The detailed working principle of IRIS is described elsewhere.[17,20] Briefly, IRIS measures the change in protein mass density on the sensor surface that has a single silicon oxide layer on silicon by utilizing optical interferometry. Protein microarray images are acquired by a CCD camera, and each pixel is fitted to the reflection function that is approximated with the equation

$$R = |r|^2 = \frac{r_1^2 + r_2^2 + 2r_1r_2\cos(2\phi)}{r_1^2r_2^2 + 2r_1r_2\cos(2\phi)} \quad (1)$$

where r_1 and r_2 are the Fresnel reflection coefficients of the buffer−SiO_2 and Si−SiO_2 interfaces, respectively. The optical path is described by the phase difference, ϕ, from eq 1, which is given by

$$\phi = \frac{2\pi d}{\lambda} n_{ox}\cos\theta \quad (2)$$

Here, d is the thickness of the layer (SiO_2 or SiO_2 plus the protein layer), n_{ox} is the refractive index of SiO_2, λ is the wavelength of the incident light, and θ is the angle of incidence, which is assumed to be zero. The thickness, d, is determined by minimizing the error when solving eqs 1 and 2. The measured thickness, or optical path length, is converted into mass density on the surface by using simple conversion factors determined in prior work.[21] The conversion factor for optical path length to protein mass density is 1 nm to 1.28 ng/mm^2. Dynamic measurements were acquired by assembling microarrays into a custom-made flow cell. In order to achieve maximum signal, the experiments were conducted in the reaction-limited regime,[22] and the flow rate was set to 50 μL/min. All tubings and the surfaces of the flow cell, including the microarrays, were blocked with 1% BSA for 1 h prior to all binding experiments to avoid nonspecific interactions.

Protein Microarray Fabrication. Silicon substrates with 500 nm of thermally grown oxide (Silicon Valley Microelectronics, Santa Clara, CA) were functionalized with copoly(*N*,*N*-dimethylacrylamide (DMA)−acryloyloxysuccinimide (NAS)−3-(trimethoxysilyl)propyl methacrylate (MAPS)) polymer described in detail elsewhere.[23] Following the surface functionalization, capture antibodies were robotically spotted onto the surface at 0.5 mg/mL. Monoclonal antibodies against recombinant human IL-6, and recombinant human tumor necrosis factor alphas (TNFα) were purchased from Thermofisher Scientific (Rockford, IL). Rabbit IgG (rIgG) and antihuman serum albumin (anti-HSA) were purchased from Sigma-Aldrich. Antibodies for interleukine-8 (IL-8) and interleukin-10 (IL-10) were provided in the ELISA kits purchased from BioLegend (San Diego, CA). All other chemical reagents were purchased from Sigma-Aldrich unless specified. Following the antibody deposition, the samples were left in a humidity-controlled environment overnight to complete the immobilization process. On the following day, the protein arrays were

dx.doi.org/10.1021/la400982h | *Langmuir* 2013, 29, 5369−5376

washed three times in PBST (0.1% tween-20 in PBS) for 3 min (3 × 3 min) and three times in PBS for 3 min (3 × 3 min) on a rotating shaker. Then, the arrays were rinsed briefly with deionized water and dried with ultrapure argon gas.

Cytokine Detection in Saline Solution and Cell Culture Medium. Recombinant human IL-6 was purchased from Thermofisher Scientific (Rockford, IL) and reconstituted to 20 μg/mL in PBS at pH 7.4. This stock solution was serially diluted to various concentrations ranging from 2 ng/mL to 1 μg/mL in 0.1% BSA in PBS. The sensor was equilibrated with 0.1% BSA in PBS solution for approximately an hour prior to introducing the cytokine solution. A detection antibody against IL-6 was purchased from Thermofisher Scientific (Rockford, IL), and it was diluted to 1 μg/mL in 0.1% BSA in PBS. For binding experiments using cell culture medium, stock solutions of IL-6 and detection antibody were diluted to 1 μg/mL in DMEM (Gibco, Life Technologies, Grand Island, NY) containing 10% fetal bovine serum, 2 mM L-glutamine, 100 U/mL penicillin, and 100 μg/mL streptomycin. For testing multiplexed nonspecific binding of mass tags, matched antibody pairs for anti-IL-8 and anti-IL-10 from BioLegend (San Diego, CA) were used. Provided concentrations of the stock solution of anti-IL-8 and anti-IL-10 by the manufacturer were 200×.

Dynamic Data Processing and Analysis. Mechanical movement of a microarray during an experiment with flowing solutions can cause fluctuations in the spatial locations of individual sensors (antibody spots) with respect to the imaging camera. Thus, postprocessing software is needed to account for the micromotion of the sensor. Initially, images taken from a binding experiment were aligned to allow identified sensors to be analyzed. However, interpolation artifacts from rotational image registration made precise quantification of small changes of mass density difficult. To address this, a robust spot finding algorithm was developed and used to locate and quantify every spot for each time point during an experiment.

We specified a number of parameters initially including the approximate baseline height difference as well as minimum radius and symmetry of the sensor. The subsequent time point calculations were automated to reduce variability introduced by user's subjectivity in sensor identification. An example of the spot finder algorithm's identified features is shown in Figure 2. The difference in the average values of the background to the sensor is used to calculate a sensor height that can then be converted to a mass density. Additionally, because dirt, salt, or other artifacts can dramatically influence label-free measurements, the software eliminated any pixels that are outside calculated standard deviations of the fitted images. In this work, pixels that had a fitting error outside one standard deviation relative to the fitting error of the entire sensor were not used for determining the average value inside a specified area. After identification of each individual sensor, the software proceeded to quantify the signal changes for each time point in a given experiment. Using the center of the sensor as a starting point, the algorithm located a new center at every time point and then calculated a signal change. If the sensor could not be identified for a particular time point, which can occur during real-time experiments because of air bubbles or other flow artifacts, it was removed for that particular time point. Pseudo code for the spot tracking algorithm is provided in the Supporting Information.

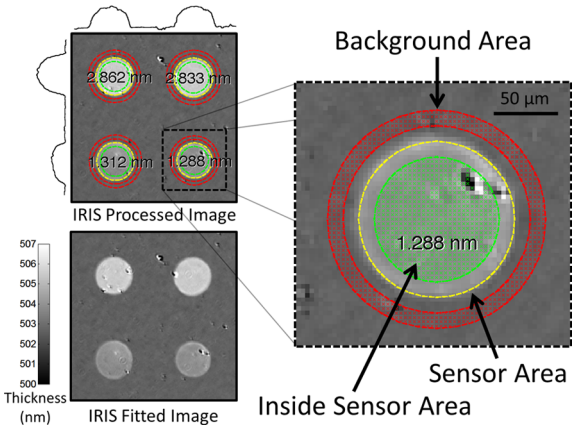

Figure 2. Example of sensors located with a robust spot finder algorithm. Processing the original image, in the bottom left, begins with accumulating the vertical and horizontal lines, as shown on the top and left of the processed image, to identify potential sensor locations. The center and radius for each sensor are then found and are used for finding the sensor signal (shown in a yellow dotted line). The zoom box illustrates the pixels used for the inside (using 80% of the radius, shown in green) and background areas (120−140% of the radius, shown in red). For accurate analysis, the dark pixels inside the sensor are excluded from height calculations. If these dark pixels were included in this example, it would result in a loss of over 10% of the calculated height.

3. RESULTS AND DISCUSSION

Characterization of the Surface Antibody Desorption. The change in surface density of the spotted antibodies on the protein microarray was monitored with IRIS while the sensor was subjected to regular binding conditions. Images were acquired approximately every 5 min while 0.1% BSA in PBS without any analyte was flowed over the sensor surface at room temperature. Antibodies on the sensor surface were steadily washed off the surface, and the amount of the surface probe loss was quantified with IRIS as shown in Figure 3. Although most

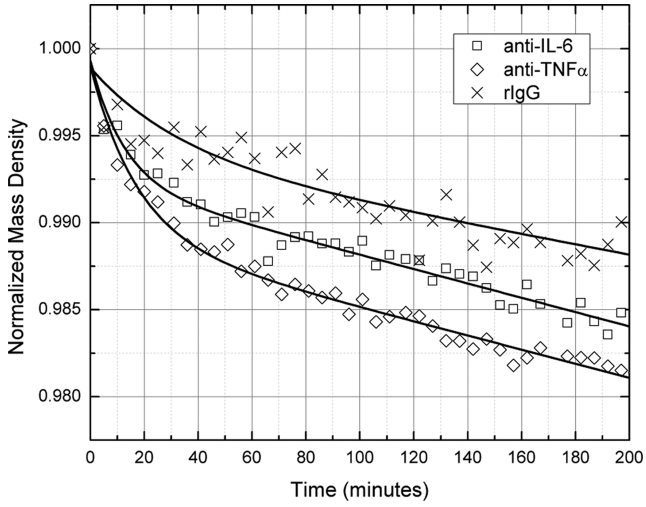

Figure 3. Surface antibody desorption kinetics. Surface mass density of the immobilized antibodies is observed with IRIS. The signal is normalized to the initial mass density of each antibody spot. The double-exponential decay function, $y = A_1e^{-k_1t} + A_2e^{-k_2t}$, is fitted and shown as the solid line.

of the antibodies on the surface are covalently bound to the polymeric network of copoly(DMA-NAS-MAPS) on the glass surface, it is reasonable to assume that a small population of the surface antibodies remained nonspecifically adsorbed after the standard wash protocol. Thus, we suspect that the initial probe loss during a flow experiment was due to washing off of the noncovalently adsorbed antibodies to the polymer layer.

Investigation of the surface probe loss was repeated over four additional trials, each with a new protein array, to examine the reproducibility of the desorption rate among arrays. All data sets were fitted to the double-exponential decay function $y = A_1e^{-k_1t} + A_2e^{-k_2t}$. The double-exponential decay model is commonly used for protein interactions in solid phase

dx.doi.org/10.1021/la400982h | Langmuir 2013, 29, 5369−5376

Table 1. Decay Constants and Time Constants of Immobilized Antibody Spots[a]

	k_1 (10^{-2} min^{-1})	k_2 (10^{-5} min^{-1})	k_1^{-1} (min)	k_2^{-1} (days)
anti-IL-6	7.29 ± 2.16	5.19 ± 2.04	13.7 ± 4.06	13.4 ± 5.26
anti-TNFα	4.98 ± 1.00	4.58 ± 1.06	20.1 ± 4.03	15.2 ± 3.51
rIgG	5.66 ± 2.63	2.41 ± 0.98	17.7 ± 8.21	28.8 ± 11.7

[a]Surface antibody desorption of five protein arrays was characterized. Each array had 10 replicate spots for different antibodies. Mean ±1 standard deviation is shown.

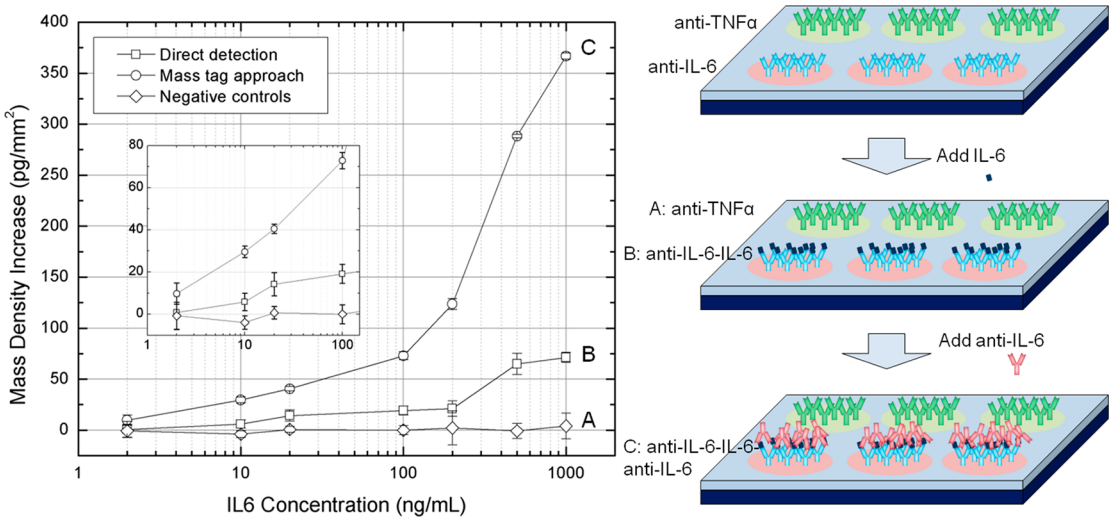

Figure 4. Dilution curve for IL-6 detection. Mass density changes at equilibrium from seven dilution experiments are plotted. Curve A is the response of negative control spots (anti-TNFα antibody) when different concentrations of IL-6 was introduced to the sensor. Curve B is the response of anti-IL-6 antibody spots and describes the direct detection of IL-6. Following the addition of IL-6, mass tag molecules, anti-IL-6 antibodies (1 μg/mL), are introduced to the sensor in every binding experiment. Curve C shows the response of anti-IL-6 antibody spots after introducing the mass tag molecules. A portion of the dilution curve at low IL-6 concentration is blown up and shown as the inset. IL-6 concentration of 19 ng/mL is detectable for direct detection, and IL-6 concentration of 2.7 ng/mL is detectable using mass tagging approach.

assays[24−27] attributing to multiple affinities of protein to the surface, and we find the double-exponential function to fit well with the observed desorption. Fitted decay constants and the corresponding time constants are shown in Table 1. It is interesting to note that the two decay terms dominate very different time scales. The smaller time constants ($1/k_1$) for all of the antibodies are less than 20 min. We suspect this initial probe loss is caused by desorption of the residual noncovalently adsorbed protein layer. The much larger time constants ($1/k_2$) can be attributed to multiple factors. It was previously shown that silica glass can dissolve in PBS at a very slow rate of 5 pm/h.[18] This slow and continuous loss of surface silica is likely one of the causes for the slow signal reduction. Furthermore, loss of surface silica causes the polymeric network that links the antibodies to the sensor surface to desorb[18] and consequently leads to the loss of capture antibodies. We observe similar protein desorption kinetics when the sensor was under a constant buffer flow for 3 days as shown in the Supporting Information (Figure S1).

Optical label-free sensors are often limited by drift rather than the noise of the system.[28] Slight changes in temperature, buffer compositions, and instabilities of the light sources can cause the signal to drift. We eliminate the possibility of these factors causing the small but continuous loss of signal we report here. First, unlike evanescent wave sensors, IRIS is independent of temperature.[17] Second, the refractive index of the bulk solution remains constant throughout the investigation. Third, fluctuations of the illumination power supply are corrected by the use of self-reference region on the sensor[29] for every image. Fourth, any uneven spatial illumination across the sensor is accounted for by normalizing the imaging field of view with a mirror under the same flow condition prior to every experiment. Lastly, any mechanical drift of the sensor surface in the flow cell relative to the optical system is ignored as individual sensors are found and analyzed for every time point with the spot tracking algorithm described above. Therefore, we conclude the decreasing optical density is caused by physical loss of biomolecules on the sensor surface.

The quantification of the surface probe loss provides extremely valuable information for investigating binding events where the protein of interest is much smaller than the size of the capturing antibody. Albeit the amount of antibody desorption is very small (1−2% of its initial amount during a 3 h period), it is comparable to the expected mass increase of the much smaller cytokines upon binding. Thus, it is critical to account for desorption of the surface antibody for cytokine detection to avoid false negative signals. At low target concentrations, the binding signal can be buried in the noise if probe loss is not accounted for as shown in the Supporting Information (Figure S2). For the binding experiments, the target cytokine was introduced ~60 min (over 3 times the small time constant, $1/k_1$) after the flow was initiated to ensure >95% desorption of the loosely bound antibodies prior to the binding event. To account for the additional and continuous probe loss, we found the rate of protein desorption of each probe type for individual experiments and subtracted it from the acquired signal.

dx.doi.org/10.1021/la400982h | Langmuir 2013, 29, 5369−5376

IL-6 Detection and Signal Amplification with Anti-IL-6 Antibody. The limit of detection for IL-6 was determined through a series of dilution experiments as follows. The protein arrays were prepared in an identical fashion as the ones used for probe loss experiments, and the same flow rate and buffer solution were used as well. Prior to introducing the target molecules to the sensor surface, 0.1% BSA in PBS was flowed over the sensor surface for ~60 min as previously discussed. Seven separate binding experiments were performed with varying concentration of IL-6 (2, 10, 20, 100, 200, 500, and 1000 ng/mL). The target solution was flowed over the sensor surface for >40 min to ensure equilibrium was reached, followed by addition of anti-IL-6 antibody (1 μg/mL) that recognized a different epitope. Both capture anti-IL-6 antibody and detection anti-IL-6 antibody were tested in a separate experiment, and they did not display any cross-reactivity. Images during a 20 min period following the equilibrium were averaged, and the changes in mass density due to binding are plotted in a dilution curve as presented in Figure 4. An anti-TNFα antibody was used as a negative control, and no cross-reactivity was observed. The analytical limit of detection (LOD) was determined as the mean blank signal, where the analyte concentration was 0, plus three standard deviations. The corresponding minimum IL-6 concentration was found by linear regression analysis in the linear region of the binding curves (R^2 = 0.989), and LOD for direct detection of IL-6 was achieved at 19 ng/mL IL6 concentration. The sensitivity improved 7-fold when the signal was enhanced with the sandwiching antibody, and LOD is reached at 2.7 ng/mL IL-6 concentration (R^2 = 0.897). The noise under flow was 16.5 pm per spot, and averaging 8 spots with the same probe reduced the noise to 3.85 pm, corresponding to protein surface density of 4.6 pg/mm^2. The noise floor is defined as the RMS (quadratic mean) around the average signal of 20 measurements. Finally, a sigmoidal dose–response curve was fitted to determine dissociation constant, K_D, at 6.0 nM.

Onsager coefficient of mass transport, L_m, was calculated to determine the influence of mass transport on the obtained results using the flowing equation:

$$L_m = 0.98\sqrt[3]{\frac{D^2 f}{h^2 b l}} \quad (3)$$

where D is the diffusion coefficient, f the flow rate, h the channel height, b the width, and l the distance from the flow cell entrance.[28] We assumed diffusion coefficient of 1.22 × 10^6 cm^2/s based on the hydrodynamic radius of IL-6,[30] which agrees well with the reported diffusion coefficients of similarly sized protein.[31,32] Considering the geometry of the flow cell (f = 50 μL/min, h = 200 μm, b = 10 mm, l = 5 mm), we obtain L_m = 1.8 × 10^{-6} m/s. This value is much greater than the product of the apparent associate rate constant and the free binding site (8.4 × 10^{-8} m/s), which indicates the kinetics were reaction limited and were free from mass transport concerns.[33] Thus, we assume a simple biomolecular interaction

$$Ab + Ag \rightleftarrows Ab{\cdot}Ag \quad (4)$$

where Ab is the amount of free surface antibodies and Ag is the amount of antigen. Data points were fitted using the least-squares method to the exponential binding curve, and k_{obs} values were obtained. Association rate (k_a) and dissociation rate (k_d) were found using initial rate analysis,[34] and they were k_a = (9.3 ± 2.1) × 10^4 M^{-1} s^{-1} and k_d = (3.7 ± 2.2) × 10^{-4} s^{-1} given that $k_{obs} = k_a[Ag]_0 + k_d$. On the basis of the kinetic analysis, we obtain K_D = 4.0 ± 2.5 nM, which is comparable to the thermodynamic K_D obtained at equilibrium.

Detection of IL-6/Anti-IL-6 Antibody Complex. Although the sandwich assay described above does not involve conventional labeling of the target molecules, the signal enhancement due to the additional antibody is essentially an amplification technique by increasing the mass of the target molecules on the surface through a specific antibody–antigen interaction. This sequential addition of mass tag requires capturing predetermined amounts of analytes prior to introduction of the mass tag, which limits the temporal resolution of the study to the number of samples collected at different time points. However, this limitation can be overcome if the mass of the target molecules is amplified prior to being captured on the surface. Approximately 130 ng/mL of IL-6 was reacted with 1 μg/mL of detection anti-IL-6 antibody (150 kDa) in 0.1% BSA in PBS solution prior to being flowed over the sensor surface. The interaction between IL-6 and the detection anti-IL-6 antibody is assumed to occur much more rapidly as it takes place in the solution than the interaction between IL-6 and the capture anti-IL-6 antibody on the planar surface. Figure 5 illustrates the successful detection of IL-6/anti-IL-6 antibody complex. Having the mass tagging molecules present in the analyte solution resulted in a 7-fold signal enhancement compared to the direct detection of IL-6 at the same concentration based on the dilution curve (Figure 4). The observed signal enhancement agrees well with the theoretical value as there is a 7-fold increase in mass of the IL-6/anti-IL-6 antibody complex relative to IL-6. Figure 5 compares the kinetics and the signal intensity of complex detection to

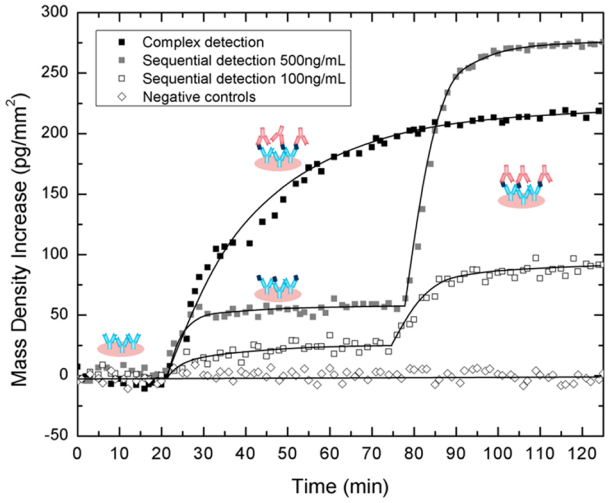

Figure 5. IL-6/anti-IL-6 antibody complex detection. Mass tag molecules, anti-IL-6 (1 μg/mL), were added to the IL-6 solution (130 ng/mL) before the analyte solution was introduced to the sensor array. For comparison, the mass density increase where the analytes (gray squares: [IL-6] = 500 ng/mL; white squares: [IL-6] = 100 ng/mL) followed by the mass tags is shown. Analytes are introduced at t = 20 min. k_{obs} = 6.9 × 10^{-4} s^{-1} for complex detection, k_{obs} = 9.8 × 10^{-4} s^{-1} for 100 ng/mL IL-6 detection, and k_{obs} = 2.6 × 10^{-3} s^{-1} for 500 ng/mL IL-6 detection. Stepwise increase in signal upon capturing the mass tags are shown around time = 75 min for sensitivity enhancement through sequential detection of mass tags. White diamonds are the signal from anti-TNFα antibody spots. Solid lines are guides for the eye.

dx.doi.org/10.1021/la400982h | Langmuir 2013, 29, 5369–5376

separate experiments where the detection anti-IL-6 antibody (1 μg/mL) was introduced following IL-6 detection with the analyte concentration at 100 and 500 ng/mL. Elimination of the separate amplification step provides the potential to detect cytokines as they are secreted by cells in real time, since the mass tags could be added in excess to the cell culture solution, thus "preamplifying" the signal.

Cytokine Detection in Complex Biological Fluid. Successful dynamic label-free detection of cytokines in complex biological fluids enables the possibility of investigating cytokine production in real time. As a proof of concept, we examine the feasibility of detecting cytokines secreted by cells with IRIS by demonstrating IL-6 detection in a standard cell culture media with 10% serum. Similar to the binding experiments carried out in PBS, media was flowed over the sensor surface for ~60 min to allow loosely bound antibodies to wash off and to obtain the protein desorption behavior prior to the addition of the cytokine. Sequential detection of IL-6 (1 μg/mL) and anti-IL-6 antibody (1 μg/mL) in cell culture medium is shown in Figure 6. High concentration of protein (3–5 mg/mL) and glucose

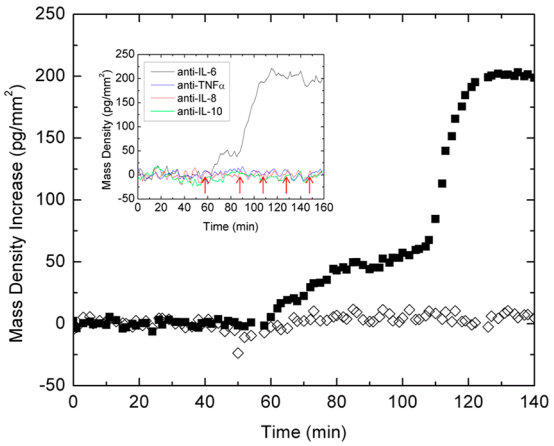

Figure 6. IL-6 detection in cell culture medium. Direct detection of IL-6 at 1 μg/mL and the subsequent detection of mass tags at 1 μg/mL are shown (closed squares). Response of anti-TNFα is shown as the negative control (open diamonds). All flow conditions were identical to the binding experiments performed in saline solution. Inset: response of an antibody array that consisted anti-IL-6, anti-TNFα, anti-IL-8, and anti-IL-10 when multiple protein targets were introduced. The red arrows mark when the target solutions were introduced in the following order: IL-6, anti-IL-6, anti-TNFα, anti-IL-8, and anti-IL-10.

(4.5 mg/mL) present in the cell culture medium did not display any nonspecific interactions with the sensor surface. We achieved a comparable noise floor to the binding experiments performed in PBS. The noise floor in the complex biological fluid was 18.7 pm per spot, and averaging 9 spots resulted in noise floor of 2.35 pm, corresponding to protein surface density of 2.8 pg/mm^2. In a separate experiment, we explored the feasibility of multiplexed cytokine detection in complex biological fluid by examining nonspecific binding of multiple mass tags on an antibody array. The array consisted of 10 replicate spots of anti-IL-6, anti-IL-8, anti-IL-10, and anti-TNFα. Resulting signals from IRIS is shown as the inset of Figure 6. Following the addition of IL-6 (1 μg/mL) and anti-IL-6 (1 μg/mL) to the array, antibodies for TNFα (50 μg/mL), IL-8 (1 × concentration), and IL-10 (1 × concentration) that are matched to the surface capture antibodies were introduced (red arrows). Nonspecific binding of mass tags onto the array in culture media was not observed. The noise floor during the entire experiment for each antibody was 7.7 pg/mm^2 (anti-IL-6), 7.4 pg/mm^2 (anti-IL-8), 8.5 pg/mm^2 (anti-IL-10), and 6.8 pg/mm^2 (anti-TNFα). Comparable noise floors from multiple antibody spots against various mass tags in complex biological fluid to the noise in PBS is a promising indication that the presented technology can be used for multiplexed detection of cell secretion.

4. CONCLUSION

We addressed the challenges of real-time quantitative detection of cytokines in an array format utilizing the quantitative nature of the interferometric reflectance imaging sensor (IRIS). Real-time characterization of the capture probes (an antibody array) spotted on the sensor surface revealed slow and continuous surface antibody desorption under constant flow. We demonstrated that the accuracy and sensitivity of IRIS can be significantly improved with a detailed understanding of the temporal behavior of surface bound probes. In turn, we achieved high sensitivity detection of cytokines.

An accurate understanding of the surface antibody desorption is particularly important for accurate and quantitative detection of smaller target molecules with larger capture probes (antibodies) as in the case of cytokine detection. For example, a 2% protein desorption of an antibody spot with the surface density of 4.4 ng/mm^2, a typical immobilization density on copoly(DMA-MAS-MAPS) functionalized surface, is equivalent to 88 pg/mm^2 of signal loss if the temporal behavior of the probes is not accounted for. This error is large enough to negate the signal upon capturing IL-6 even at a high concentration (500 ng/mL). In our experiments, accurate probe characterization led to a LOD of ~19 ng/mL. A further improvement of sensitivity was demonstrated by inclusion of detection antibodies as mass tags. More significantly, we showed that the detection antibody molecules for signal enhancement do not interfere with the IRIS signal and thus can be present in the target solution eliminating the need of separate washing and tagging steps. In this approach, detection antibodies acting as mass tags are mixed with the target solution containing the cytokines and the antibody–cytokine complexes are captured on the sensor surface. This technique resulted in more than 7-fold signal improvement in detecting small protein with the expected limit of detection approaching 2 ng/mL. While the use of mass tags is similar to labeling approaches, the advantage of this technique over conventional labeling methods is that it offers dynamic detection capability of a label-free biosensor. In addition, unlike other label-free biosensors with comparable sensitivity, IRIS signal is independent of the bulk solution compositions, allowing mass amplification during target detection. Therefore, this technique enables IRIS to study kinetics of cytokine secretion. As the first step toward that effort, the ability to detect cytokines in cell culture medium is demonstrated with a comparable noise floor. We plan to develop a cell–antibody dual array for IRIS to capture cytokines directly adjacent to the cells as they are secreted. The estimated cost of maintaining the mass tags in the culture media for immediate mass amplification is $7.50 for a 24 h period, which is not a limiting cost factor for implementing this technique. Because IRIS can be highly multiplexed, and the sensors are easy to fabricate at a minimum cost, IRIS can be used as a platform for *in vitro* study of pathogen/immunological response, drug response, or disease progression through real-

dx.doi.org/10.1021/la400982h | *Langmuir* 2013, 29, 5369–5376

time quantitative monitoring of multiple cytokines or other proteins secreted by cells.

■ ASSOCIATED CONTENT

Supporting Information

Pseudo code for the spot finding algorithm, long-term protein desorption kinetics, and the effects of probe loss correction in accurate and quantitative detection. This material is available free of charge via the Internet at http://pubs.acs.org.

■ AUTHOR INFORMATION

Corresponding Author

*E-mail selim@bu.edu, Tel +1 (617) 353-5067, Fax +1 (617) 353-6440.

Notes

The authors declare no competing financial interest.

■ ACKNOWLEDGMENTS

We thank Alexander Reddington for maintaining IRIS for dynamic detection. The financial support for this work was provided by Boston University Center for Nanoscience and Nanobiotechnology, National Institute of Health, under R21EB015900-02, and Boston Urban Fellows Program funded via National Science Foundation GK-12 Project (Award # 0538608).

■ REFERENCES

(1) Medzhitov, R. Origin and physiological roles of inflammation. *Nature* **2008**, *454* (7203), 428−435.

(2) Szelenyi, J. Cytokines and the central nervous system. *Brain Res. Bull.* **2001**, *54* (4), 329−38.

(3) Krueger, J. M.; Obal, F. J.; Fang, J.; Kubota, T.; Taishi, P. The role of cytokines in physiological sleep regulation. *Ann. N.Y. Acad. Sci.* **2001**, *933*, 211−21.

(4) Hopkins, S. J. The pathophysiological role of cytokines. *Leg. Med.* **2003**, *5 (Suppl.)*, S45−57.

(5) Byrd, J. C.; Murphy, T.; Howard, R. S.; Lucas, M. S.; Goodrich, A.; Park, K.; Pearson, M.; Waselenko, J. K.; Ling, G.; Grever, M. R.; Grillo-Lopez, A. J.; Rosenberg, J.; Kunkel, L.; Flinn, I. W. Rituximab using a thrice weekly dosing schedule in B-Cell chronic lymphocytic leukemia and small lymphocytic lymphoma demonstrates clinical activity and acceptable toxicity. *J. Clin. Oncol.* **2001**, *19* (8), 2153−2164.

(6) Ishihara, K.; Hirano, T. IL-6 in autoimmune disease and chronic inflammatory proliferative disease. *Cytokine Growth Factor Rev.* **2002**, *13* (4−5), 357−368.

(7) O'Shea, J. J.; Ma, A.; Lipsky, P. Cytokines and autoimmunity. *Nat. Rev. Immunol.* **2002**, *2* (1), 37−45.

(8) Salazar-Onfray, F.; Lopez, M. N.; Mendoza-Naranjo, A. Paradoxical effects of cytokines in tumor immune surveillance and tumor immune escape. *Cytokine Growth Factor Rev.* **2007**, *18* (1−2), 171−182.

(9) Dranoff, G. Cytokines in cancer pathogenesis and cancer therapy. *Nat. Rev. Cancer* **2004**, *4* (1), 11−22.

(10) La Belle, J. T.; Bhavsar, K.; Fairchild, A.; Das, A.; Sweeney, J.; Alford, T. L.; Wang, J.; Bhavanandan, V. P.; Joshi, L. Cytokine immunosensor for multiple sclerosis detection based upon label-free electrochemical impedance spectroscopy. *Biosens. Bioelectron.* **2007**, *23* (3), 428−431.

(11) Battaglia, T. M.; Masson, J. F.; Sierks, M. R.; Beaudoin, S. P.; Rogers, J.; Foster, K. N.; Holloway, G. A.; Booksh, K. S. Quantification of cytokines involved in wound healing using surface plasmon resonance. *Anal. Chem.* **2005**, *77* (21), 7016−7023.

(12) Stybayeva, G.; Kairova, M.; Ramanculov, E.; Simonian, A. L.; Revzin, A. Detecting interferon-gamma release from human CD4 T-cells using surface plasmon resonance. *Colloids Surf., B* **2010**, *80* (2), 251−255.

(13) Washburn, A. L.; Luchansky, M. S.; Bowman, A. L.; Bailey, R. C. Quantitative, label-free detection of five protein biomarkers using multiplexed arrays of silicon photonic microring resonators. *Anal. Chem.* **2010**, *82* (1), 69−72.

(14) Luchansky, M. S.; Bailey, R. C. Silicon photonic microring resonators for quantitative cytokine detection and T-cell secretion analysis. *Anal. Chem.* **2010**, *82* (5), 1975−1981.

(15) Kyo, M.; Usui-Aoki, K.; Koga, H. Label-free detection of proteins in crude cell lysate with antibody arrays by a surface plasmon resonance imaging technique. *Anal. Chem.* **2005**, *77* (22), 7115−7121.

(16) Qavi, A. J.; Washburn, A. L.; Byeon, J. Y.; Bailey, R. C. Label-free technologies for quantitative multiparameter biological analysis. *Anal. Bioanal. Chem.* **2009**, *394* (1), 121−35.

(17) Ozkumur, E.; Needham, J. W.; Bergstein, D. A.; Gonzalez, R.; Cabodi, M.; Gershoni, J. M.; Goldberg, B. B.; Unlu, M. S. Label-free and dynamic detection of biomolecular interactions for high-throughput microarray applications. *Proc. Natl. Acad. Sci. U. S. A.* **2008**, *105* (23), 7988−7992.

(18) Ahn, S.; Spuhler, P. S.; Chiari, M.; Cabodi, M.; Ünlü, M. S. Quantification of surface etching by common buffers and implications on the accuracy of label-free biological assays. *Biosens. Bioelectron.* **2012**, *36* (1), 222−229.

(19) Monroe, M. R.; Reddington, A. P.; Collins, A. D.; LaBoda, C.; Cretich, M.; Chiari, M.; Little, F. F.; Unlu, M. S. Multiplexed method to calibrate and quantitate fluorescence signal for allergen-specific IgE. *Anal. Chem.* **2011**, *83* (24), 9485−9491.

(20) Daaboul, G. G.; Vedula, R. S.; Ahn, S.; Lopez, C. A.; Reddington, A.; Ozkumur, E.; Ünlü, M. S. LED-based interferometric reflectance imaging sensor for quantitative dynamic monitoring of biomolecular interactions. *Biosens. Bioelectron.* **2011**, *26* (5), 2221−2227.

(21) Ozkumur, E.; Yalcin, A.; Cretich, M.; Lopez, C. A.; Bergstein, D. A.; Goldberg, B. B.; Chiari, M.; Unlu, M. S. Quantification of DNA and protein adsorption by optical phase shift. *Biosens. Bioelectron.* **2009**, *25* (1), 167−172.

(22) Parsa, H.; Chin, C. D.; Mongkolwisetwara, P.; Lee, B. W.; Wang, J. J.; Sia, S. K. Effect of volume- and time-based constraints on capture of analytes in microfluidic heterogeneous immunoassays. *Lab Chip* **2008**, *8* (12), 2062−2070.

(23) Cretich, M.; Pirri, G.; Damin, F.; Solinas, I.; Chiari, M. A new polymeric coating for protein microarrays. *Anal. Biochem.* **2004**, *332* (1), 67−74.

(24) O'Shannessy, D. J.; Brighamburke, M.; Soneson, K. K.; Hensley, P.; Brooks, I. Determination of rate and equilibrium binding constants for macromolecular interactions using surface-plasmon resonance - Use of nonlinear least-squares analysis-methods. *Anal. Biochem.* **1993**, *212* (2), 457−468.

(25) Schuck, P. Kinetics of ligand binding to receptor immobilized in a polymer matrix, as detected with an evanescent wave biosensor. 1. A computer simulation of the influence of mass transport. *Biophys. J.* **1996**, *70* (3), 1230−1249.

(26) Khan, F.; He, M. Y.; Taussig, M. J. Double-hexahistidine tag with high-affinity binding for protein immobilization, purification, and detection on Ni-nitrilotriacetic acid surfaces. *Anal. Chem.* **2006**, *78* (9), 3072−3079.

(27) O'Shannessy, D. J. Determination of kinetic rate and equilibrium binding constants for macromolecular interactions: a critique of the surface plasmon resonance literature. *Curr. Opin. Biotechnol.* **1994**, *5* (1), 65−71.

(28) Haake, H. M.; Schutz, A.; Gauglitz, G. Label-free detection of biomolecular interaction by optical sensors. *Fresenius J. Anal. Chem.* **2000**, *366* (6−7), 576−585.

(29) Vedula, R.; Daaboul, G.; Reddington, A.; Ozkumur, E.; Bergstein, D. A.; Unlu, M. S. Self-referencing substrates for optical interferometric biosensors. *J. Mod. Opt.* **2010**, *57* (16), 1564−1569.

(30) Kimmel, J. D.; Gibson, G. A.; Watkins, S. C.; Kellum, J. A.; Federspiel, W. J. IL-6 adsorption dynamics in hemoadsorption beads

studied using confocal laser scanning microscopy. *J. Biomed. Mater. Res., Part B: Appl. Biomater.* **2010**, *92B* (2), 390−396.
(31) de la Torre, J. G.; Huertas, M. L.; Carrasco, B. Calculation of hydrodynamic properties of globular proteins from their atomic-level structure. *Biophys. J.* **2000**, *78* (2), 719−730.
(32) Walters, R. R.; Graham, J. F.; Moore, R. M.; Anderson, D. J. Protein diffusion-coefficient measurements by laminar-flow analysis - method and applications. *Anal. Biochem.* **1984**, *140* (1), 190−195.
(33) Glaser, R. W. Antigen-antibody binding and mass-transport by convection and diffusion to a surface - a 2-dimensional computer-model of binding and dissociation kinetics. *Anal. Biochem.* **1993**, *213* (1), 152−161.
(34) Edwards, P. R.; Leatherbarrow, R. J. Determination of association rate constants by an optical biosensor using initial rate analysis. *Anal. Biochem.* **1997**, *246* (1), 1−6.